Supporting Information

Fluorescence Switch Based on NIR-emitting Carbon Dots Revealing Multi-resistance in the Rapid Response and Cell Bioimaging of Oxytetracycline

Muhammad Muzammal Hussain, Fengli Li, Farid Ahmed, Waheed Ullah Khan and Hai Xiong*

Institute for Advanced Study, Shenzhen University, Shenzhen, 518060, China

*Corresponding author: hai.xiong@szu.edu.cn

Materials and characterization

1,5-diaminonaphthalene and ammonium citrate were purchased from Macklin (Shanghai China), whereas other neutral analytes such as Kanamycin, Methionine, chloramphenicol, ampicillin, arabinose, spectinomycin, glucose, lysine, melamine, cysteine, glutathione, and oxytetracycline were purchased from Adamas Reagents Co., Ltd. All chemicals purchased from commercial sources and are analytical grade. The UV-Visible (UV-vis) spectra were acquired using a UV-2600 spectrophotometer (Shimadzu), while the fluorescence spectra were measured utilizing an F-7000 FL spectrophotometer (HITACHI). The particle size and morphology of NIR-CDs were analyzed via a high-resolution transmission electron microscope (HR-TEM, F-200), and Fourier transformed infrared (FTIR) spectrum using FT-IR Spectrometer (PerkinElmer) was used to explore the presence of different functional groups. The elemental composition of the synthesized nanoprobe was determined through X-ray photoelectron spectroscopy (XPS) using a Thermo Fisher Scientific ESCALAB 250Xi microprobe equipped with a monochromatic Al K-alpha source (1361 eV). The hydrogen nuclear magnetic resonance (^{1}H-NMR) spectrum was obtained using a Bruker 400 NMR spectrometer.

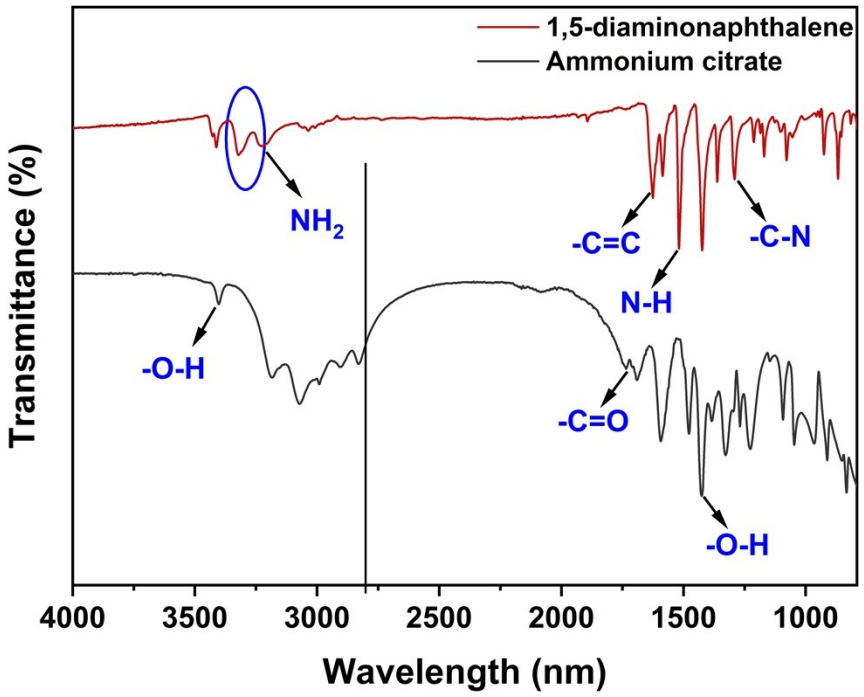

Fig. S1 FTIR Spectra of precursors.

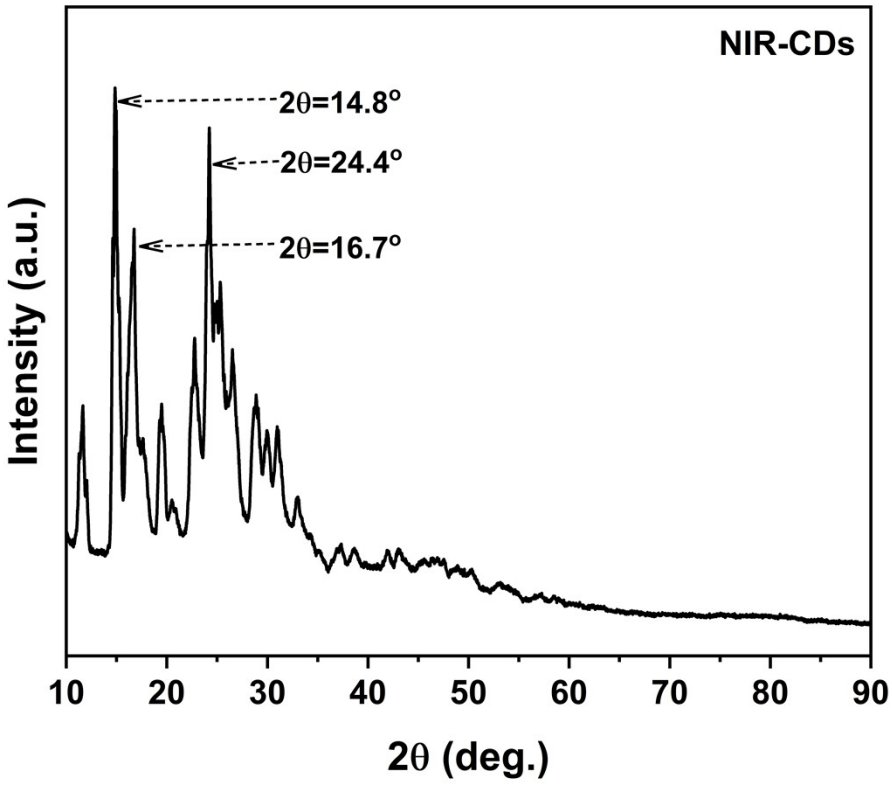

Fig. S2 XRD Spectrum of synthesized NIR-CDs.

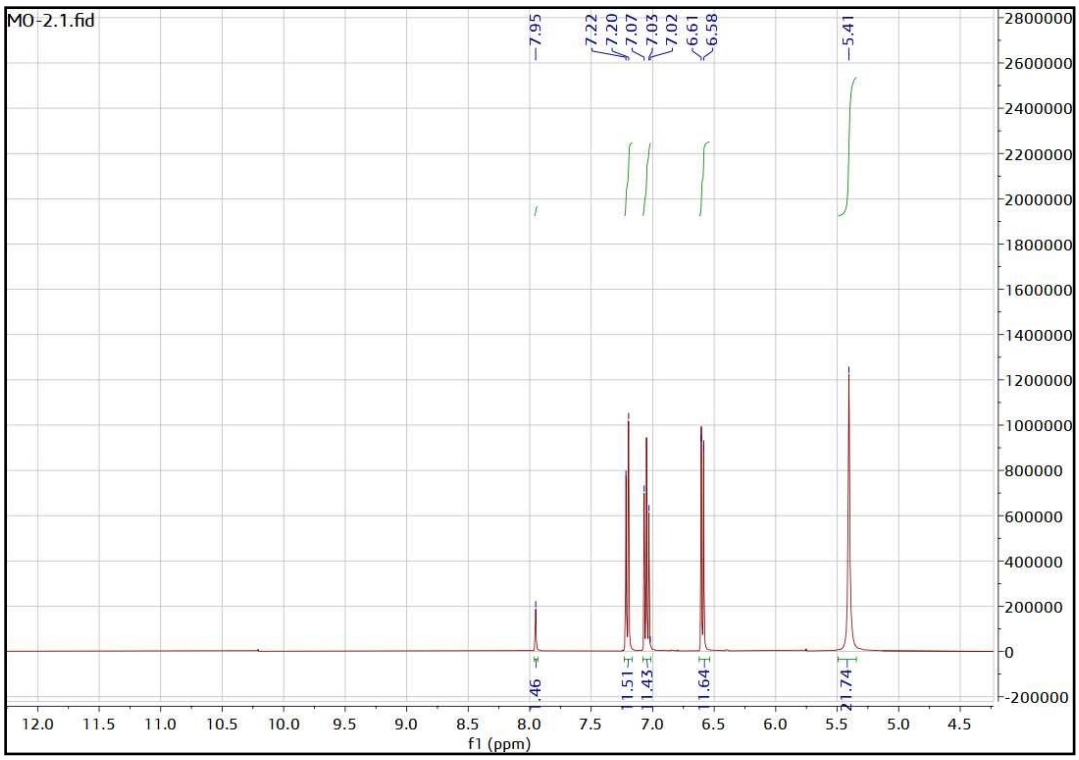

Fig. S3 ^{1}H-NMR spectrum of NIR-CDs solution in DMSO.

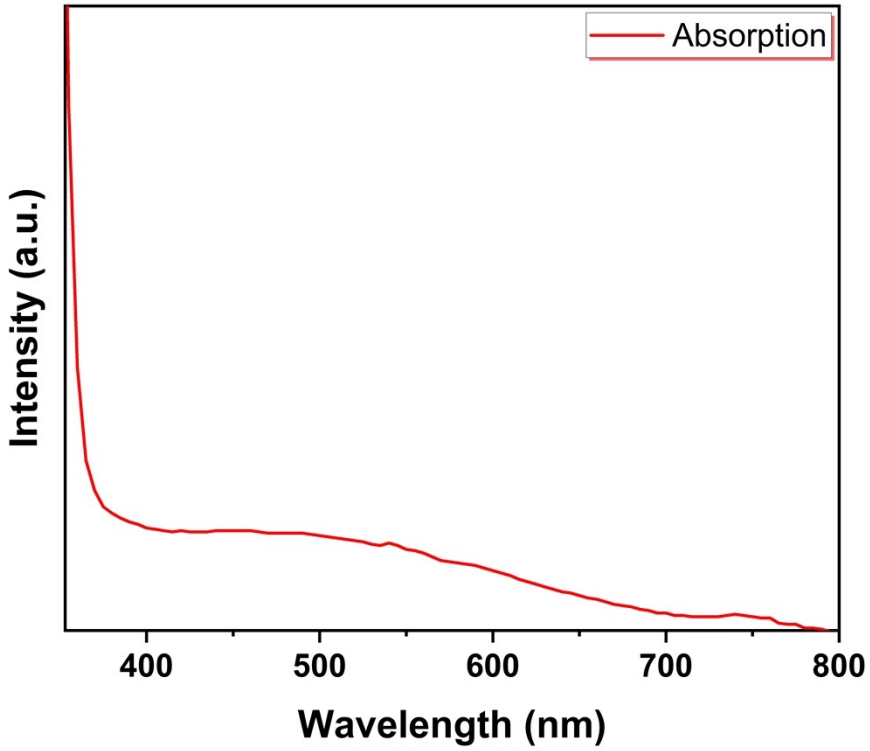

Fig. S4 Absorption spectrum of NIR-CDs.

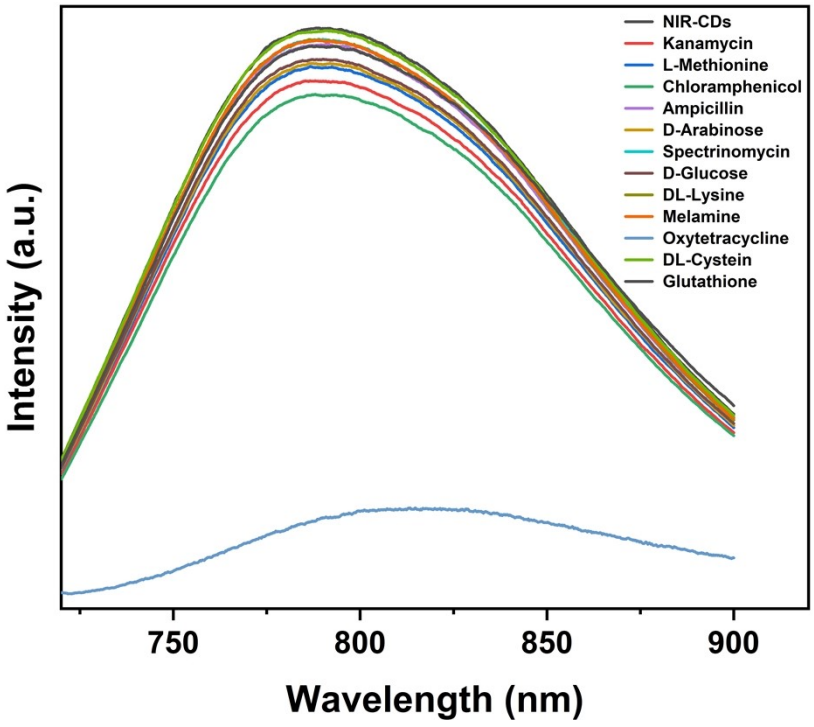

Fig. S5 Change of FL intensity for NIR-CDs upon interaction with various biomolecules (100 μM).

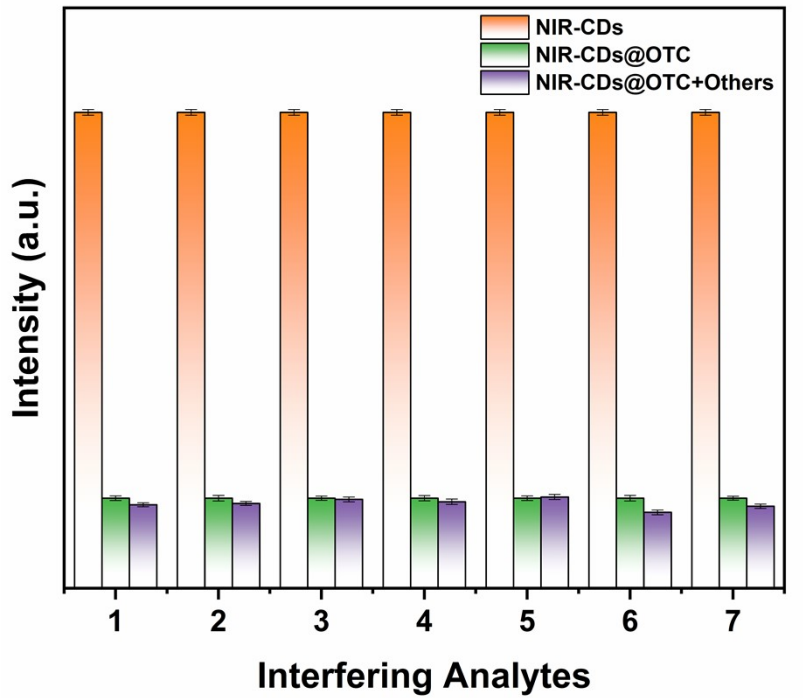

Fig. S6 Selectivity of NIR-CDs towards OTC in the presence of different anions and antibiotics: 1=Cl^-, 2= CO_3^-, 3= NO_3^-, 4= SO_4^-, 5=CH_3COO^-, 6=Tetracycline, and 7=Doxycycline.

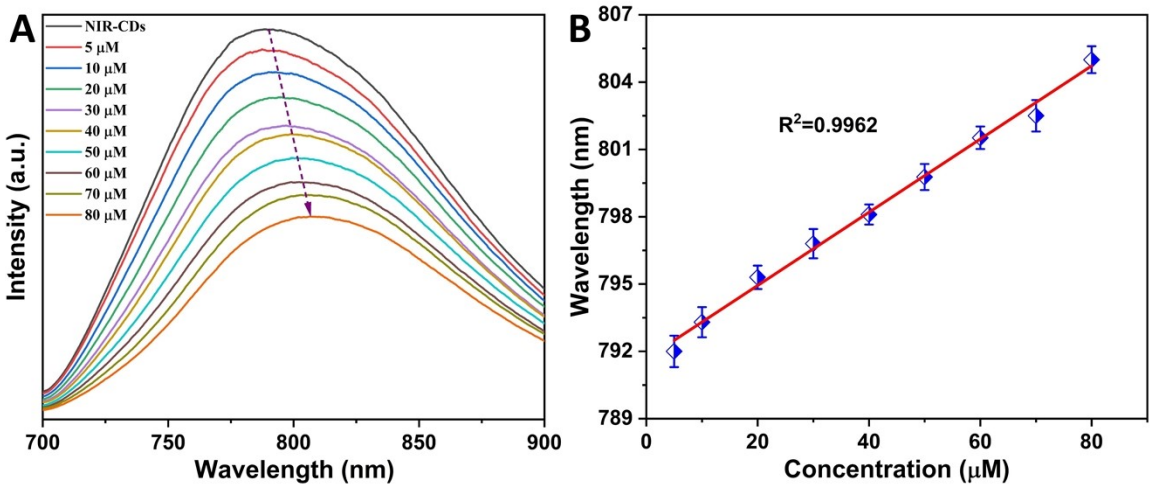

Fig. S7 (A) Peak shift towards NIR region upon the interaction of CDs with different concentrations of OTC (5-80 µM). (B) Linear response calibration of peak shift towards NIR-II region on different concentrations of OTC.

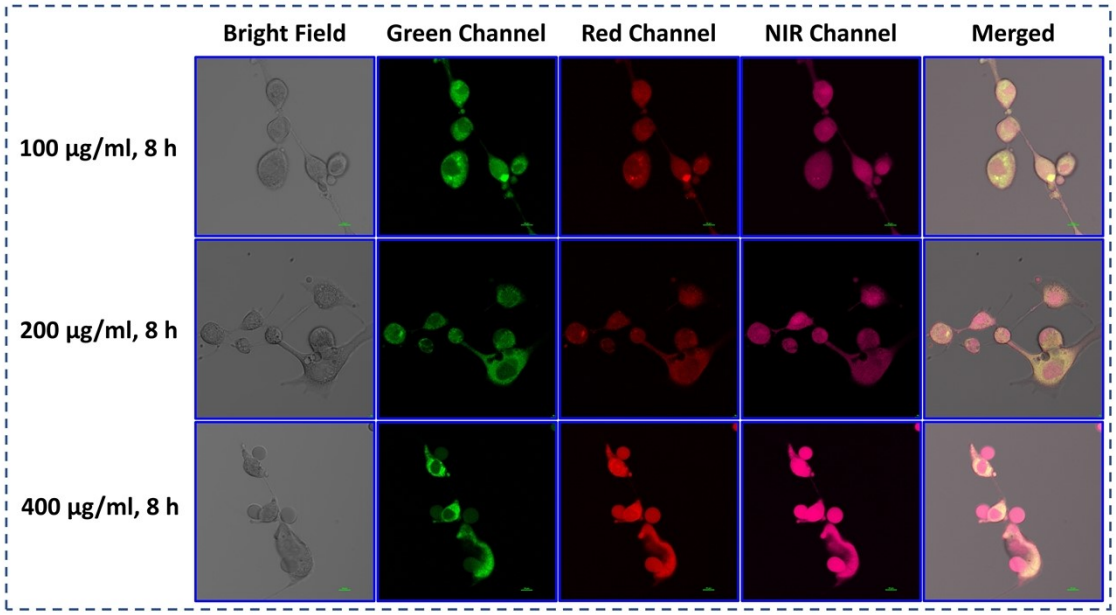

Fig. S8 Different concentrations of NIR-CDs at 8 h constant incubation time.

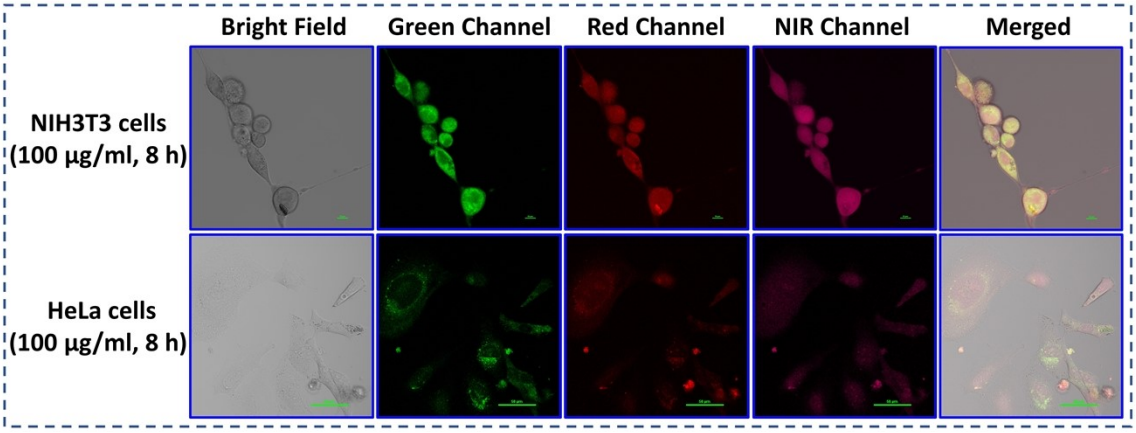

Fig. S9 Fluorescence with optimized conditions in NIH3T3 and HeLa cells.

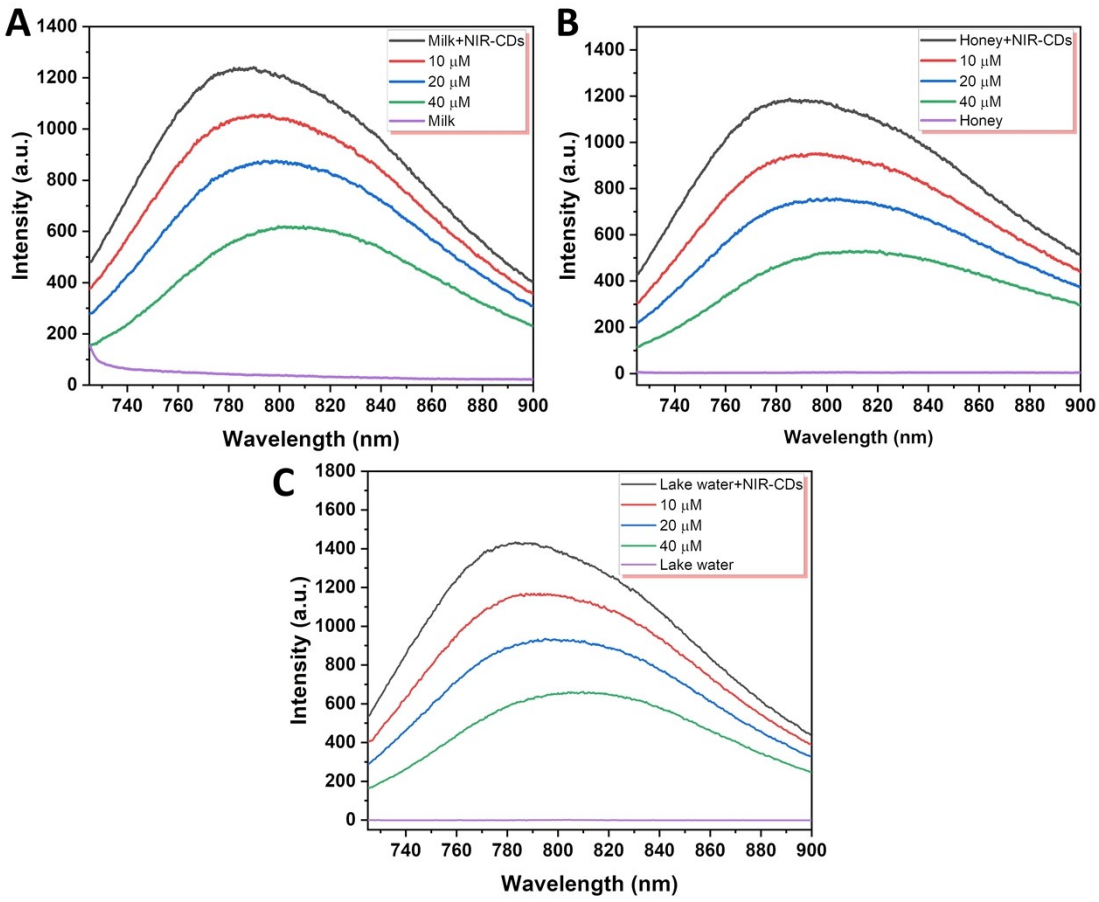

Fig. S10 Real sample detection in (A) Milk. (B) Honey. (C) Lake water.

Table S1 A summary of synthesis and fluorescence properties of NIR-CDs.

Nr.	Method	Precursors	E_x/E_m(nm)	Quantum yield (%)	Ref.
1	oxidative polymerization/hydrotherm	Polythiophene phenylpropionic acid	600/800	2.3 (water)	[1]
2	Electrochemical etching	Graphite rods	500/610	1.8	[2]
3	Hydrothermal synthesis	PT2, diphenyl diselenide, NaOH	460/731, 820	0.2 (water)	[3]
4	Hydrothermal synthesis	Polythiophene derivatives	530/700	3.92 (water)	[4]
5	Hydrothermal synthesis	Watermelon juice	808/925	0.4	[5]
6	Solvothermal synthesis	Manganese (II) phthalocyanine	690/745	-	[6]
7	Hydrothermal synthesis	1,5-diaminonaphthelene, ammonium citrate	705/790	1.8 (water)	This work

Table S2 Performances of CDs based methods applied for various detection of TCs.

Method	Linear Range (μM)	LOD (μM/L)	Sample type	RSD (%)	Recovery (%)	Ref.
N-CQDs/Fe^{3+} (IFE)	3.32-32.3	0.74	River water, tap water	<1.32	96.9	[7]
CDs@MOF(Eu) (FRET)	0-200	0.36	TBS buffer solution	<1.41	93.9-102	[8]
Eu-CQDs (IFE)	0.500–200	0.30	Running water, lake water	<3.00	92.4-110	[9]
CQDs	10-400	6	-	-	-	[10]
MIPs@AA-CQDs	1.00-60.0	0.17	River water	-	96.0-105	[11]
CD-SAM/GO (IFE)	4.76-9.90	0.928	Milk	<4.55	99.8-101	[12]
NCDs (IFE)	0-30	0.07	Lake/tap water	<3.50	98.6-108	[13]
S, N-CQDs	1.88-60	0.56	Milk, honey, tap water	<3.52	93.61-102.31	[14]
NIR-CDs	5-80	0.11	Milk, honey, lake water	<1.8	83.38-111.67	This work

References

1. J. Ge, Q. Jia, W. Liu, L. Guo, Q. Liu, M. Lan, H. Zhang, X. Meng and P. Wang, *Adv. Mater.*, 2015, **27**, 4169-4177.
2. X. Tan, Y. Li, X. Li, S. Zhou, L. Fan and S. Yang, *Chem. Commun.*, 2015, **51**, 2544-2546.
3. M. Lan, S. Zhao, Z. Zhang, L. Yan, L. Guo, G. Niu, J. Zhang, J. Zhao, H. Zhang, P. Wang, G. Zhu, C. Lee and W. Zhang, *Nano Res.*, 2017, **10**, 3113-3123.
4. D. Huang, H. Zhou, Y. Wu, T. Wang, L. Sun, P. Gao, Y. Sun, H. Huang, G. Zhou and J. Hu, *Carbon*, 2019, **142**, 673-684.
5. Y. Li, G. Bai, S. Zeng and J. Hao, *ACS Appl. Mater. Interfaces*, 2019, **11**, 4737-4744.
6. Q. Jia, J. Ge, W. Liu, X. Zheng, S. Chen, Y. Wen, H. Zhang and P. Wang, *Adv. Mater.*, 2018, **30**, 1706090.
7. H. Qi, M. Teng, M. Liu, S. Liu, J. Li, H. Yu, C. Teng, Z. Huang, H. Liu, Q. Shao, A. Umar, T. Ding, Q. Gao and Z. Guo, *J. Colloid Interface Sci.*, 2019, **539**, 332-341.
8. X. Fu, R. Lv, J. Su, H. Li, B. Yang, W. Gu and X. Liu, *RSC Adv.*, 2018, **8**, 4766-4772.
9. O. S. Ahmad, T. S. Bedwell, C. Esen, A. Garcia-Cruz and S. A. Piletsky, *Trends Biotechnol.*, 2019, **37**, 294-309.
10. Y. Yan, J. H. Liu, R. S. Li, Y. F. Li, C. Z. Huang and S. J. Zhen, *Anal. Chim. Acta*, 2019, **1063**, 144-151.
11. X. Wei, L. Lv, Z. Zhang and W. Guan, *J. Appl. Polym. Sci.*, 2020, **137**, 49126.
12. B. Al-Hashimi, K. M. Omer and H. S. Rahman, *Arab. J. Chem.*, 2020, **13**, 5151-5159.
13. S. Jayaweera, K. Yin and W. J. Ng, *J. Fluoresc.*, 2019, **29**, 221-229.
14. Y. Fan, W. Qiao, W. Long, H. Chen, H. Fu, C. Zhou and Y. She, *Spectrochim. Acta A Mol. Biomol. Spectrosc.*, 2022, **274**, 121033.